

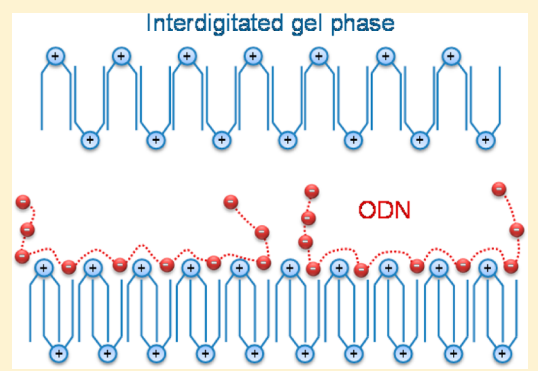
Oligonucleotide Adsorption Affects Phase Transition but Not Interdigitation of diC14-Amidine Bilayers

Julio H. K. Rozenfeld,^{*,†} Evandro L. Duarte,[†] Tiago R. Oliveira,[†] Caroline Lonez,[‡] Jean-Marie Ruysschaert,[‡] and M. Teresa Lamy[†]

[†]Instituto de Física, Universidade de São Paulo, São Paulo, Brazil

[‡]Service de Structure et Fonction des Membranes Biologiques, Université Libre de Bruxelles, Bruxelles, Belgium

ABSTRACT: In this work, we investigate the effect of a small single-stranded oligonucleotide (ODN) on the colloid stability and structure of cationic diC14-amidine liposomes. Dynamic light scattering (DLS) shows that small, stable, anionic assemblies are formed in presence of excess ODN negative charge. This charge overcompensation condition was further characterized. A less cooperative bilayer phase transition is observed by differential scanning calorimetry (DSC). Electron spin resonance (ESR) spectra of probes at different bilayer depths show that ODN electrostatic adsorption increases the rigidity of both interdigitated gel and lamellar fluid phases. The increase in gel phase rigidity could be explained by the transformation of an adjacent to an interpenetrated interdigitation. Interdigitated fusogenic bilayers may find interesting applications in delivery of therapeutic oligonucleotides.



1. INTRODUCTION

Oligonucleotides have been extensively used in basic research of gene expression and function,^{1,2} vaccine design,³ and allergy⁴ and cancer therapy.⁵ Several oligonucleotide-based formulations have reached the clinical trial phase⁶ and one is already on the market.⁷ All these applications, however, are dependent on suitable carriers that protect oligonucleotides against degradation and improve their capture by target cells.^{8,9}

The cationic lipid diC14-amidine efficiently delivers nucleic acids to mammalian cells.^{10,11} It was recently shown that diC14-amidine bilayers present an interdigitated phase which strongly correlates with a potent fusogenic activity at low temperatures.^{12,13}

Interdigitated phases correspond to very ordered gel phases where the two bilayer leaflets are merged; they usually result from perturbations at the interfacial region such as modifications of the polar headgroup area or dehydration of the bilayer.¹⁴ Interdigitation has been described for asymmetric lipids or mixed-chain lipids of different chain lengths^{15–17} and for lipids with large effective headgroup sizes.^{18,19} It has also been described for symmetric lipids under pressure modifications^{20,21} or in the presence of alcohol,^{22–24} glycerol,²⁵ acetonitrile,¹⁴ polymyxin B,²⁵ or ions like thiocyanate.²⁶ Surprisingly, the role of polyelectrolytes on membrane interdigitation has been only poorly investigated.²⁷

In the present work, we use dynamic light scattering (DLS), differential scanning calorimetry (DSC), and electron spin resonance (ESR) to explore the effect of a small single-stranded oligonucleotide (ODN) polyelectrolyte on the structure and colloid stability of interdigitated diC14-amidine membranes.

2. MATERIALS AND METHODS

2.1. Reagents. diC14-amidine (3-tetradecylamino-*N*-*tert*-butyl-*N'*-tetradecyl-propionamidine) was synthesized as described¹¹ and stored as a powder at -20°C . The chemical structure of diC14-amidine is shown in Figure 1. Ten-base single-stranded oligonucleotide 3'-AAA AAA AAA A-5' (ODN) was purchased from Integrated DNA Technologies IDT (Coralville, IA, USA). Hepes (4-(2-hydroxyethyl)-piperazine-1-ethanesulfonic acid) was purchased from Sigma Chemical Co. (St. Louis, MO, USA). Spin labels 1-palmitoyl-2-(*n*-doxylsearoyl)-*sn*-glycero-3-phosphocholine (*n*-PCSL, *n* = 5, 7, 12, or 16) were supplied by Avanti Polar Lipids (Birmingham, AL, USA). Ultrapure water of Milli-Q-Plus quality was used throughout.

2.2. Preparation of Liposomes and Liposome/ODN Assemblies. A lipid film was formed from a chloroform solution, dried under a stream of N_2 , and left under reduced pressure for a minimum of 2 h, to remove all traces of organic solvent. Dispersions were prepared by addition of Hepes buffer (10 mM, pH 7.4) followed by vortexing for about 2 min above T_m ($\sim 40^{\circ}\text{C}$). For ESR experiments, spin labels were added to the lipid chloroform solution at 0.2 mol % relative to the lipid concentration in order to avoid any spin–spin interactions.

Assemblies were prepared by adding suitable volumes of ODN stock solutions prepared in Hepes buffer (10 mM, pH 7.4) to the liposomes. Final lipid concentrations were 0.2 mM, 2 mM, and 10 mM for DLS, DSC, and ESR experiments, respectively. A fixed 1:5 ODN:diC14-amidine molar ratio was used for DSC and ESR experiments. The higher lipid concentration for ESR experiments improved the signal-to-noise ratio during spectra acquisition. Assemblies were allowed to incubate at room temperature for 24 h and were agitated on a vortex immediately before the experiments in order to ensure homogeneity.

Received: April 29, 2013

Revised: June 22, 2013

Published: August 8, 2013

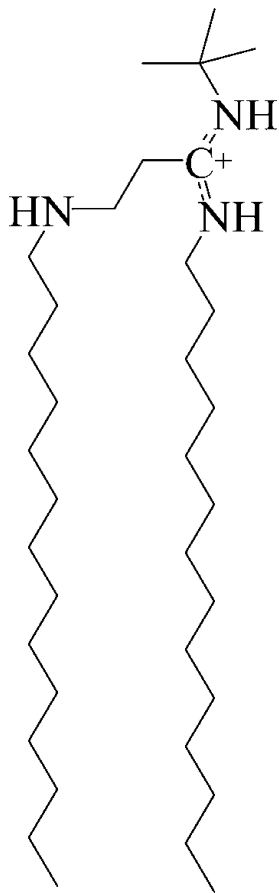


Figure 1. Chemical structure of diC14-amidine.

2.3. Determination of Dispersions Zeta-Average Diameter and Zeta-Potential. Zeta-average (mean hydrodynamic) diameter (D_z) and zeta-potential (ζ) of dispersions were determined by dynamic light scattering (DLS) using a ZetaSizer Nano (Malvern Instruments Ltd., Worcestershire, UK) equipped with a 633 nm laser. ζ was determined from the electrophoretic mobility μ and Smoluchowski equation, $\zeta = \mu\eta/\epsilon$, where η and ϵ are medium viscosity and dielectric constant, respectively. D_z and ζ represent mean values of at least 10 independent measurements and experiments were performed at 25 °C.

2.4. Differential Scanning Calorimetry (DSC). DSC scans were performed in a Microcal VP-DSC Microcalorimeter (Microcal Inc., Northampton, MA, USA) equipped with 0.5 mL twin total-fill cells. Heating rates were 20 °C/h. Scans were performed at least in duplicate. The enthalpy of transition ΔH was obtained by integrating the area under the thermograms.

2.5. Electron Spin Resonance (ESR) Spectroscopy. ESR measurements at X-band were performed with a Bruker EMX spectrometer. Field-modulation amplitude of 1G and microwave power of 5 mW were used. The temperature was controlled to about 0.2 °C with a Bruker BVT-2000 variable temperature device, and monitored with a Fluke 51 K/J thermometer with a probe placed just above the cavity. A high sensitivity ER4119HS cavity was used. All ESR data shown are means of the results of at least two experiments, and the uncertainties are the standard deviations. When not shown, the uncertainty was found to be smaller than the symbol in the graph.

The effective order parameter, S_{eff} was calculated from the expression²⁵

$$S_{\text{eff}} = \frac{A_{\parallel\parallel} - A_{\perp\perp}}{A_{zz} - (1/2)(A_{xx} + A_{yy})} \frac{a'_o}{a_o}$$

where $a'_o = (1/3)(A_{xx} + A_{yy} + A_{zz})$; $a_o = (1/3)(A_{\parallel\parallel} + 2A_{\perp\perp})$; $A_{\parallel\parallel}$ (= A_{max}) is the maximum hyperfine splitting directly measured in the

spectrum (see Figure 7); $A_{\perp\perp} = A_{\text{min}} + 1.4\{1 - [(A_{\parallel\parallel} - A_{\text{min}})/(A_{zz} - (1/2)(A_{xx} + A_{yy}))]\}$; A_{min} is the measured minimum hyperfine splitting (see Figure 7); and A_{xx} , A_{yy} , and A_{zz} are the principal values of the hyperfine tensor for doxylpropane.²⁸ The ratio between the low and central field line amplitudes (h_+ / h_0) was also directly taken from spectra (see Figure 7).

3. RESULTS AND DISCUSSION

3.1. Effect of ODN on Colloid Stability of diC14-Amidine Liposomes. The effect of ODN concentration on colloid stability of 0.2 mM diC14-amidine liposomes is shown in Figure 2. Addition of ODN to the small (~100 nm) and

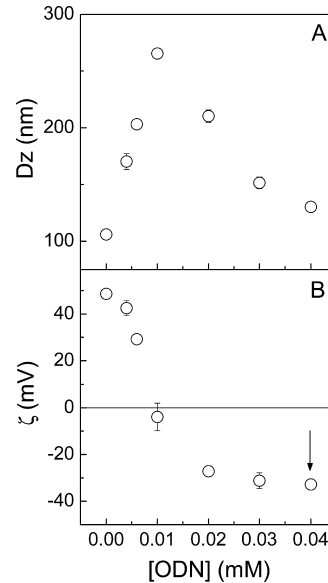


Figure 2. Effect of ODN concentration on zeta-average diameter (A) and zeta-potential (B) of 0.2 mM diC14-amidine liposomes. Arrow indicates the 1:5 ODN:diC14-amidine molar proportion chosen for DSC and ESR experiments.

cationic liposomes led to a simultaneous increase in zeta-average diameters and decrease in zeta-potentials (Figure 2A and B). At 0.01 mM ODN, diameters reached a maximum of 265 nm and the net charge of assemblies was close to zero (isoelectric point).

Above 0.01 mM ODN, diC14-amidine/ODN assemblies were negatively charged and diameters decreased reaching a plateau around 0.04 mM ODN (Figure 2A and B). An unstable region around the isoelectric point was observed: reversible aggregation and precipitation took place in the range of 0.006–0.02 mM ODN during the period of incubation prior to experiments. For this reason, samples were agitated on a vortex prior to experiments, as described in Material and Methods.

The non-monotonic behavior observed in Figure 2 is typical of polyelectrolytes adsorbing to oppositely charged particles: charge neutralization leads to flocculation (and eventually fusion) and charge overcompensation leads to colloid restabilization due to recovery of the electrostatic repulsion between the assemblies.^{29–32}

The plateau of negative charge reached at 0.04 mM ODN (arrow in Figure 2B) suggests not only that all available sites for ODN binding are occupied at the bilayer surface, but also that unbound phosphate groups of adsorbed ODN molecules are exposed to the medium. The anionic, small (~130 nm), and stable assemblies obtained at this 1:5 ODN:diC14-amidine

molar ratio were chosen for further structural characterization because maximum ODN loading would be useful for biological assays.

Although cationic particles are considered as a must for gene and oligonucleotide delivery, anionic particles have been successfully employed as carriers for immune system cells.^{33–35} In fact, it was recently shown that anionic assemblies made of cationic lipid and oligonucleotides displayed enhanced immunoadjuvant activity.³⁶

3.2. Effect of ODN on diC14-Amidine Gel-Fluid Transition. The effect of ODN on the gel-fluid transition of diC14-amidine bilayers is shown in Figure 3. The phase

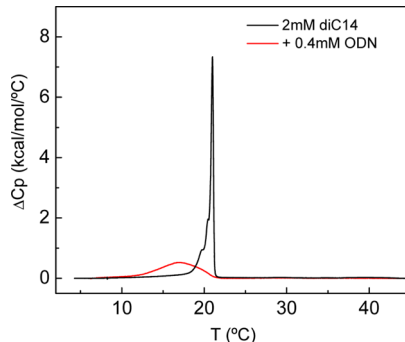


Figure 3. Effect of 0.4 mM ODN on DSC thermogram of 2 mM diC14-amidine. Scan rate was 20 °C/h.

transition of naked diC14-amidine bilayers was relatively sharp with a peak at 21 °C, as previously described.³⁷ However, in the presence of saturating ODN concentration, a much broader transition starting at lower temperatures and peaking around 17 °C was observed (Figure 3). The broadening of thermogram profile indicated that transition cooperativity was significantly reduced in presence of ODN.

The almost complete disappearance of the sharp diC14-amidine phase transition in the presence of ODN is in good agreement with previous DSC results obtained with increasing concentrations of plasmid DNA.³⁷ The bilayer phase transition is governed by both headgroup interactions and acyl chain interactions,^{38,39} and can be affected by adsorption of polyelectrolytes. In fact, superficial adsorption of anionic⁴⁰ and branched cationic⁴¹ polymers to zwitterionic dimyristoyl phosphatidylcholine (DMPC) bilayers decrease transition cooperativity, probably due to the formation of domains in the membrane.

One could argue that the adsorption of such saturating concentration of ODN could be leading to a major restructuring of the bilayer, for instance, the formation of pores or micelle-like regions. In order to gain insight into the microscopic organization of the diC14-amidine bilayers, ESR spectroscopy was employed.

3.3. Effect of ODN on Bilayer Gel Phase Structure. Phospholipids spin-labeled at different positions of the hydrocarbon chain probed the microenvironment changes caused by ODN at different depths of the diC14-amidine bilayers. Figure 4 shows the ESR spectra of 5-, 7-, 12-, and 16-PCSL inserted into the gel phase ($T = 5$ °C) of diC14-amidine membranes. The spectra in the absence and presence of ODN are very similar, showing that the bilayer structure is preserved. If more fluid regions (like pores) were formed, one would expect more isotropic spectra at both the bilayer surface and core, and/or the coexistence of typical gel and fluid phase

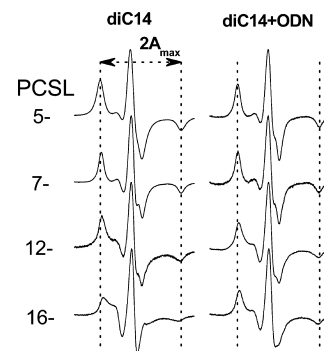


Figure 4. Effect of 2 mM ODN on ESR spectra of 5-, 7-, 12-, and 16-PCSL incorporated in 10 mM diC14-amidine liposomes at 5 °C. Dotted lines indicate the positions of the maximum hyperfine splitting (A_{\max}) on the 5-PCSL spectra. Total spectra width is 100 G.

signals.⁴² In contrast, the 16-PCSL spectrum in the presence of ODN is clearly more anisotropic than the one in naked bilayer, suggesting a more rigid bilayer core in the former (Figure 4).

In the gel phase, the maximum hyperfine splitting, A_{\max} , directly measured from the ESR spectra, is sensitive to the label microenvironment viscosity⁴³ (Figure 5). It is a measure of membrane fluidity, since both chain order and mobility parameter are evaluated.

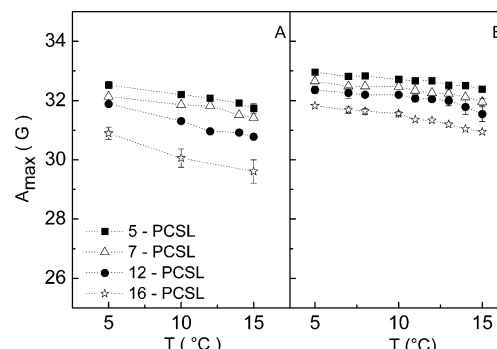


Figure 5. Maximum hyperfine splitting (A_{\max}) measured on ESR spectra of different spin labels incorporated in the gel phase of diC14-amidine liposomes (A) or ODN/diC14-amidine assemblies (B).

A recent comparison with the zwitterionic lipid DMPC, which has the same hydrophobic domain of C14 atoms chains, showed that the gel phase of diC14-amidine presented a more rigid bilayer with no fluidity gradient toward the bilayer core.¹³ This was interpreted as an interdigitated organization in the gel phase, and is consistent with A_{\max} values for diC14-amidine in the range of 29.5 G to 32.5 G (Figure 5A). Notably, in the presence of ODN, the A_{\max} values are much higher and concentrated in the narrow range between 31 and 33 G (Figure 5B), suggesting not only that the interdigitation is preserved, but also that the bilayer is even more rigid.

It was recently suggested that the interdigitated gel phase of diC14-amidine bilayers could be formed by molecules packed side by side and flipped horizontally from each other.⁴⁴ This adjacent configuration, shown in Figure 6A, would lead to a significant exposure of the hydrophobic bilayer core to the aqueous phase and could explain the very efficient fusogenic activity of diC14-amidine at low temperatures.^{13,44}

Cationic lipids presenting big headgroups and short acyl chains or high surface charge density were described to adopt

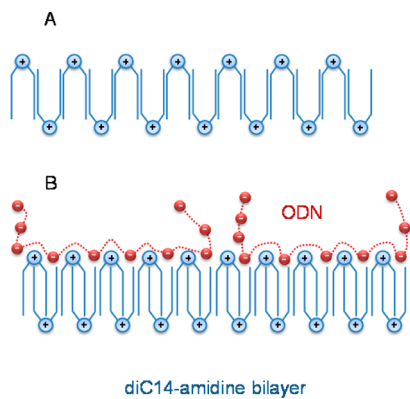


Figure 6. Scheme of adjacent (A) and interpenetrated (B) interdigitated gel phases of diC14-amidine bilayers.

an interdigitated phase.^{18,45–47} In those cases, the driving force for interdigititation was the repulsion between headgroups, caused by the net charge density of the polar heads. Indeed, neutralization of this charge by adding neutral lipids or salt affected interdigititation.⁴⁷

In the case of diC14-amidine, however, the lipid backbone appears to play a bigger role in forming an interdigitated gel phase than the headgroup: the larger separation of the myristic chains due to their connection to “extra” NH groups (Figure 1) would explain why interdigititation is observed in diC14-amidine but not in dimyristoyl phosphatidylglycerol (DMPG), a hydrocarbon chain analogue with a larger charged headgroup.^{44,48}

It is noteworthy that the rigidity of the amidine bilayer is kept even at 15 °C (Figure 5B), a temperature where phase transition is starting to take place (Figure 3). The increase in rigidity of the gel phase accompanied by a less cooperative phase transition could be attributed either to partial penetration of ODN into the bilayer or to electrostatic interactions affecting the hydrocarbon chains interactions.

If ODN penetration should occur, one would expect modifications in the spectra of spin-labels near the bilayer surface. For instance, in the case of α -MSH, a cationic peptide that partially penetrates anionic DMPG bilayers, a small decrease in the bilayer packing of the region probed by 5-PCSL was observed.⁴⁹ The increase in A_{\max} values for 5- and 7-PCSL shows that ODN actually increased superficial bilayer packing (Figure 5B). Furthermore, fluorescence assays demonstrated that the bulky adenine purine rings, such as the ones used in the present work, hindered the approach of oligonucleotide phosphates toward cationic DOTAP headgroups.⁵⁰ Consistently, oligonucleotides did not affect ESR spectra of bilayer surface probes for DOTAP/DOPE and DC-Chol/DOPE cationic liposomes.^{51,52}

The shielding of electrostatic repulsion between cationic headgroups by negatively charged phosphates of adsorbed ODN molecules could be responsible for the increase in bilayer rigidity. In this case, ODN adsorption could lead to a change in conformation of the interdigitated phase: instead of having horizontally flipped molecules side by side, one of the two acyl chains would interdigitate into the space between chains of the opposing lipid (Figure 6B).

This interpenetrated (rather than adjacent) configuration would better shield the hydrophobic region from the aqueous phase (Figure 6A and B). It would also render the ODN adsorption more energetically favorable, because the highly

organized interfacial water bound around the apolar moieties of the bilayer could be easily removed. In fact, it is known that ODN adsorption causes dehydration of the water–lipid interface in a concentration-dependent manner.⁵³ Most important of all, the interpenetrated conformation would explain how it is possible to increase rigidity of an already rigid interdigitated bilayer (Figure 5).

The diC14-amidine gel bilayer is clearly more rigid in the presence of ODN (Figure 5), though the oligonucleotide considerably decreases the phase transition cooperativity (Figure 3). Though apparently contradictory, these two experimental results can be rationalized if one has in mind that the gel–fluid thermal transition is dependent on both headgroup and acyl chain interactions.^{38,39} As discussed in the previous section, polyelectrolyte adsorption can decrease phase transition cooperativity due to the formation of domains.^{40,41} This effect might be further enhanced considering that, at the saturating ODN concentration used here (Figure 2B), there are negatively charged unbound phosphate groups at the bilayer surface, strongly attached to the membrane by adsorbed ODN moieties. The electrostatic repulsion between these negative overhangs could be responsible for the early start of the bilayer gel–fluid transition as well as contribute to the substantial decrease in its cooperativity.

3.4. Effect of ODN on the Bilayer Fluid Phase. Figure 7 shows the ESR spectra of 5-, 7-, 12-, and 16-PCSL inserted into the fluid phase ($T = 40$ °C) of diC14-amidine membranes in the absence or presence of ODN. Spectra profiles indicate that bilayer packing decreases toward the bilayer core for both samples, as expected for lamellar fluid phases. However, spectra in the presence of ODN seem more anisotropic, especially the 5- and 7-PCSL cases, indicating a more packed fluid phase for diC14-amidine bilayers in the presence of ODN (Figure 7).

For the fluid phase, distinct parameters have to be used to analyze spectra of the different spin labels. The effective order parameter (S_{eff}) is an appropriate parameter to evaluate acyl chain order with the 5- and 7-PCSL probes. Due to the position of the nitroxide group closer to the bilayer surface, in an

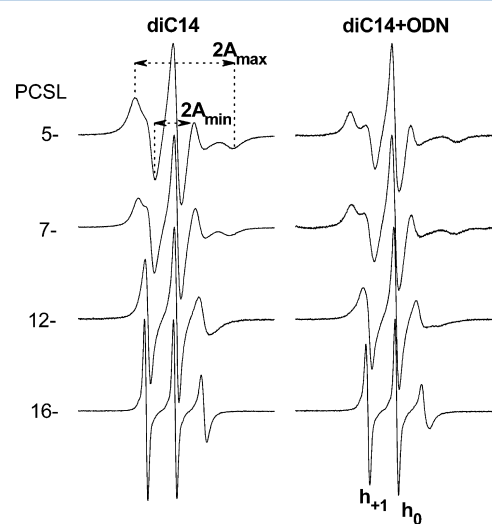


Figure 7. Effect of 2 mM ODN on ESR spectra of 5-, 7-, 12-, and 16-PCSL incorporated in 10 mM diC14-amidine liposomes at 40 °C. Maximum and minimum hyperfine splitting (A_{\max} and A_{\min}) are indicated, as well as the position of low (h_{+1}) and central (h_0) field lines. Total spectra width is 100 G.

ordered microenvironment, their ESR spectra are anisotropic, and both the maximum and minimum hyperfine splitting (A_{\max} and A_{\min} , respectively), can be directly measured, as shown in Figure 7. As described in Materials and Methods, calculated S_{eff} values depend on both A_{\max} and A_{\min} values.⁵⁴ S_{eff} includes contributions from chain order, but the main contribution is the amplitude of segmental motion of the acyl chains.⁵⁴

Spin labels located deeper in the bilayer, such as 12- and 16-PCSL, sense a less ordered microenvironment and yield more isotropic signals from which A_{\max} and A_{\min} cannot be accurately measured. However, the ratio of the amplitudes of the central and low field lines (h_{+1} and h_0 are indicated in Figure 7) can be evaluated accurately. The h_{+1}/h_0 amplitude ratio tends to unity as the spin label mobility increases.⁵⁵ S_{eff} and h_{+1}/h_0 amplitude ratios for diC14-amidine bilayers in the absence or presence of ODN are shown in Figure 8.

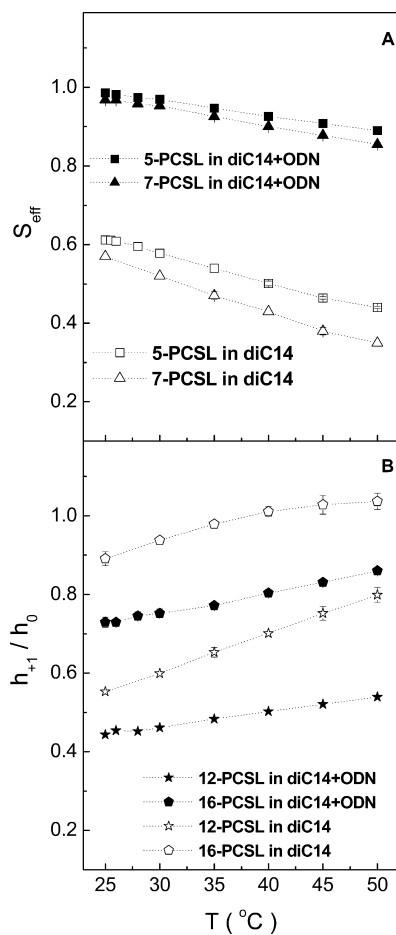


Figure 8. Effective order parameter (S_{eff}) measured on ESR spectra of 5- and 7-PCSL (A) and h_{+1}/h_0 ratios measured on ESR spectra of 12- and 16-PCSL (B) incorporated in the fluid phase of diC14-amidine liposomes (open symbols) or ODN/diC14-amidine assemblies (full symbols).

S_{eff} values increase and h_{+1}/h_0 amplitude ratios decrease in the presence of ODN (Figure 8A and B), indicating that ODN rigidifies the fluid phase both at the surface and at the core of diC14-amidine bilayers. The rigidifying effect of ODN can be attributed to the shielding of electrostatic repulsion between cationic diC14-amidine heads. A similar effect was described for diC14-amidine bilayers in the presence of long double-stranded DNA molecules, but not for single nucleotides.⁵⁶ Hence, the

polyelectrolyte character of ODN seems to be determinant in controlling the tighter packing of fluid diC14-amidine bilayers. It is interesting to observe that in the presence of such saturating ODN concentration, diC14-amidine bilayers have a transition from a very rigid interdigitated gel phase to a rigid fluid phase. That could explain why phase transition enthalpies decreased from 5.8 kcal/mol in naked diC14-amidine bilayers to 3.4 kcal/mol in the presence of ODN (Figure 3).

4. CONCLUSIONS

Small, stable, anionic assemblies were obtained from electrostatic adsorption of a single-stranded oligonucleotide onto cationic diC14-amidine liposomes. Oligonucleotide adsorption decreased bilayer phase transition temperature and cooperativity, but maintained an interdigitated gel phase.

Electrostatic interactions between negative charged oligonucleotide and cationic diC14-amidine headgroups increased the rigidity of both gel and fluid phases. The increase in gel phase rigidity was probably due to the transformation of an adjacent to an interpenetrated interdigititation induced by oligonucleotide adsorption.

Considering that diC14-amidine displays unexpected biological properties such as TLR-4 agonist activity,⁵⁷ anti-inflammatory,^{58,59} or immunomodulatory properties,⁶⁰ detailed knowledge about its structure in stable, anionic assemblies fully loaded with oligonucleotides can have great impact on future immunological applications.

■ AUTHOR INFORMATION

Corresponding Author

*Phone number: +55 11 3091 6953. E-mail address: julioroz@if.usp.br (J.H.K. Rozenfeld).

Notes

The authors declare no competing financial interest.

■ ACKNOWLEDGMENTS

This work was supported by USP, FAPESP, CNPq, and FNRS. J.H.K.R. is a FAPESP fellow (2011/13079-9). We thank Prof. Vera B. Henriques for the insightful discussions.

■ REFERENCES

- De-Backer, M. D.; Nelissen, B.; Logghe, M.; Viaene, J.; Loonen, I.; Vandoninck, S.; de-Hoogt, R.; Dewaele, S.; Simons, F. A.; Verhasselt, P.; Vanhoof, G.; Contreras, R.; Luyten, W. H. An antisense-based functional genomics approach for identification of genes critical for growth of *Candida albicans*. *Nat. Biotechnol.* **2001**, *19*, 235–241.
- Dean, N. M. Functional genomics and target validation approaches using antisense oligonucleotide technology. *Curr. Opin. Biotechnol.* **2001**, *12*, 622–625.
- Liu, L.; Zhou, X.; Liu, H.; Xiang, L.; Yuan, Z. CpG motif act as a danger signal and provides a T helper type 1-biased microenvironment for DNA vaccination. *Immunology* **2005**, *115*, 223–230.
- Fonseca, D. E.; Kline, J. N. Use of CpG oligonucleotides in treatment of asthma and allergic disease. *Adv. Drug Delivery Rev.* **2009**, *61*, 256–262.
- Kuramoto, Y.; Nishikawa, M.; Hyoudou, K.; Yamashita, F.; Hashida, M. Inhibition of peritoneal dissemination of tumor cells by single dosing of phosphodiester CpG oligonucleotide/ cationic liposome complex. *J. Controlled Release* **2006**, *115*, 226–233.
- Flaherty, K. T.; Stevenson, J. P.; O'Dwyer, P. J. Antisense therapeutics: lessons from early clinical trials. *Curr. Opin. Oncol.* **2001**, *13*, 499–505.

(7) Marwick, C. First "antisense" drug will treat CMV retinitis. *J. Am. Med. Assoc.* **1998**, *280*, 871.

(8) Shi, F.; Hoekstra, D. Effective intracellular delivery of oligonucleotides in order to make sense of antisense. *J. Controlled Release* **2004**, *97*, 189–209.

(9) Juliano, R.; Alam, M. R.; Dixit, V.; Kang, H. Mechanisms and strategies for effective delivery of antisense and siRNA oligonucleotides. *Nucleic Acids Res.* **2008**, *36*, 4158–4171.

(10) El Ouahabi, A.; Pector, V.; Fuks, R.; Vandenbranden, M.; Ruysschaert, J. M. Double long-chain amidine liposome-mediated self replicating RNA transfection. *FEBS Lett.* **1996**, *380*, 108–112.

(11) Ruysschaert, J. M.; El Ouahabi, A.; Willeaume, V.; Huez, G.; Fuks, R.; Vandenbranden, M.; Di Stefano, P. A novel cationic amphiphile for transfection of mammalian cells. *Biochem. Biophys. Res. Commun.* **1994**, *203*, 1622–1628.

(12) Lensink, M. F.; Lonez, C.; Ruysschaert, J. M.; Vandenbranden, M. Characterization of the cationic DiC(14)-amidine bilayer by mixed DMPC/ DiC(14)-amidine molecular dynamics simulations shows an interdigitated nonlamellar bilayer phase. *Langmuir* **2009**, *25*, 5230–5238.

(13) Oliveira, T. R.; Duarte, E. L.; Lamy, M. T.; Vandenbranden, M.; Ruysschaert, J. M.; Lonez, C. Temperature-dependence of cationic lipid bilayer intermixing: possible role of interdigitation. *Langmuir* **2012**, *28*, 4640–4647.

(14) Wu, F. G.; Wang, N. N.; Tao, L. F.; Yu, Z. W. Acetonitrile induces nonsynchronous interdigitation and dehydration of dipalmitoylphosphatidylcholine bilayers. *J. Phys. Chem. B* **2010**, *114*, 12685–12691.

(15) Hirsh, D. J.; Lazaro, N.; Wright, L. R.; Boggs, J. M.; McIntosh, T. J.; Schaefer, J.; Blazyk, J. A new monofluorinated phosphatidylcholine forms interdigitated bilayers. *Biophys. J.* **1998**, *75*, 1858–1868.

(16) Hui, S. W.; Mason, J. T.; Huang, C. Acyl chain interdigitation in saturated mixed-chain phosphatidylcholine bilayer dispersions. *Biochemistry* **1984**, *23*, 5570–5577.

(17) Koynova, R.; Macdonald, R. C. Mixtures of cationic lipid O-ethylphosphatidylcholine with membrane lipids and DNA: phase diagrams. *Biophys. J.* **2003**, *85*, 2449–2465.

(18) Winter, I.; Pabst, G.; Rappolt, M.; Lohner, K. Refined structure of 1,2-diacyl-P-O-ethylphosphatidylcholine bilayer membranes. *Chem. Phys. Lipids* **2001**, *112*, 137–150.

(19) Tristram-Nagle, S.; Lewis, R. N.; Blickenstaff, J. W.; Diprima, M.; Marques, B. F.; McElhaney, R. N.; Nagle, J. F.; Schneider, J. W. Thermodynamic and structural characterization of amino acid-linked dialkyl lipids. *Chem. Phys. Lipids* **2005**, *134*, 29–39.

(20) Braganza, L. F.; Worcester, D. L. Hydrostatic pressure induces hydrocarbon chain interdigitation in single-component phospholipid bilayers. *Biochemistry* **1986**, *25*, 2591–2596.

(21) Singh, H.; Emberley, J.; Morrow, M. R. Pressure induces interdigitation differently in DPPC and DPPG. *Eur. Biophys. J.* **2008**, *37*, 783–792.

(22) Rowe, E. S. Comparative effects of short chain alcohols on lipid phase transitions. *Alcohol* **1985**, *2*, 173–176.

(23) Simon, S. A.; McIntosh, T. J. Interdigitated hydrocarbon chain packing causes the biphasic transition behavior in lipid/alcohol suspensions. *Biochim. Biophys. Acta* **1984**, *773*, 169–172.

(24) Polozova, A.; Li, X.; Shangguan, T.; Meers, P.; Schuette, D. R.; Ando, N.; Gruner, S. M.; Perkins, W. R. Formation of homogeneous unilamellar liposomes from an interdigitated matrix. *Biochim. Biophys. Acta* **2005**, *1668*, 117–125.

(25) Boggs, J. M.; Rangaraj, G. Phase transitions and fatty acid spin label behavior in interdigitated lipid phases induced by glycerol and polymyxin. *Biochim. Biophys. Acta* **1985**, *816*, 221–233.

(26) Cunningham, B. A.; Tamura-Lis, W.; Lis, L. J.; Collins, J. M. Thermodynamic properties of acyl chain and mesophase transitions for phospholipids in KSCN. *Biochim. Biophys. Acta* **1989**, *984*, 109–112.

(27) Tirrell, D. A.; Turek, A. B.; Wilkinson, D. A.; McIntosh, T. J. Observation of an interdigitated gel phase in dipalmitoylphosphati-

dylglycerol bilayers treated ionene-6,6. *Macromolecules* **1985**, *18*, 1512–1513.

(28) Hubbel, W. L.; McConnell, H. M. Molecular motion in spin-labeled phospholipids and membranes. *J. Am. Chem. Soc.* **1971**, *93*, 314–326.

(29) Sybachin, A. V.; Efimova, A. A.; Litmanovich, E. A.; Menger, F. M.; Yaroslavov, A. A. Complexation of polycations to anionic liposomes: composition and structure of the interfacial complexes. *Langmuir* **2007**, *23*, 10034–10039.

(30) Sennato, S.; Bordi, F.; Cametti, C.; Diociaiuti, M.; Malaspina, P. Charge patch attraction and reentrant condensation in DNA-liposome complexes. *Biochim. Biophys. Acta* **2005**, *1714*, 1–24.

(31) Yaroslavov, A. A.; Rakhnyanskaya, A. A.; Yaroslavova, E. G.; Efimova, A. A.; Menger, F. M. Polyelectrolyte-coated liposomes: stabilization of the interfacial complexes. *Adv. Colloid Interface Sci.* **2008**, *142*, 43–52.

(32) Rozenfeld, J. H. K.; Oliveira, T. R.; Lamy, M. T.; Carmona-Ribeiro, A. M. Interaction of cationic bilayer fragments with a model oligonucleotide. *Biochim. Biophys. Acta* **2011**, *1808*, 649–655.

(33) Kazzaz, J.; Neidleman, J.; Singh, M.; Ott, G.; O'Hagan, D. T. Novel anionic microparticles are a potent adjuvant for the induction of cytotoxic T lymphocytes against recombinant p55 gag from HIV-1. *J. Controlled Release* **2000**, *67*, 347–356.

(34) Singh, M.; Kazzaz, J.; Chesko, J.; Soenawan, E.; Uguzzoli, M.; Giuliani, M.; Pizza, M.; Rappuoli, R.; O'Hagan, D. T. Anionic microparticles are a potent delivery system for recombinant antigens from *Neisseria meningitidis* serotype B. *J. Pharmaceut. Sci.* **2004**, *93*, 273–282.

(35) Singh, M.; Uguzzoli, M.; Kazzaz, J.; Chesko, J.; Soenawan, E.; Mannucci, D.; Titta, F.; Contorni, M.; Volpini, G.; Del Giudice, G.; O'Hagan, D. T. A preliminary evaluation of alternative adjuvants to alum using a range of established and new generation vaccine antigens. *Vaccine* **2006**, *24*, 1680–1686.

(36) Rozenfeld, J. H. K.; Silva, S. R.; Ranéia, P.; Faquim-Mauro, E.; Carmona-Ribeiro, A. M. Stable assemblies of cationic bilayer fragments and CpG oligonucleotide with enhanced immunoadjuvant activity in vivo. *J. Controlled Release* **2012**, *160*, 367–373.

(37) Pector, V.; Backmann, J.; Maes, D.; Vandenbranden, M.; Ruysschaert, J. M. Biophysical and structural properties of DNA-diC(14)-amidine complexes. Influence of the DNA/lipid ratio. *J. Biol. Chem.* **2000**, *275*, 29533–29538.

(38) Träuble, H.; Eibl, H. Electrostatic effects on lipid phase transitions: membrane structure and ionic environment. *Proc. Natl. Acad. Sci. U.S.A.* **1974**, *71*, 214–219.

(39) Lee, A. G. Lipid phase transitions and phase diagrams: I. Lipid phase transitions. *Biochim. Biophys. Acta* **1977**, *472*, 237–281.

(40) Feng, Z. V.; Granick, S.; Gewirth, A. A. Modification of a supported lipid bilayer by polyelectrolyte adsorption. *Langmuir* **2004**, *20*, 8796–8804.

(41) Sikor, M.; Sabin, J.; Keyvanloo, A.; Schneider, M. F.; Thewalt, J. L.; Bailey, A. E.; Frisken, B. J. Interaction of a charged polymer with zwitterionic lipid vesicles. *Langmuir* **2010**, *26*, 4095–4102.

(42) Benatti, C. R.; Feitosa, E.; Fernandez, R. M.; Lamy-Freund, M. T. Structural characterization of dioctadecyldimethylammonium bromide dispersions by spin labels. *Chem. Phys. Lipids* **2001**, *111*, 93–104.

(43) Freed, J. H. (1976) in *Spin labeling: Theory and Applications*, Berliner, L. J., Ed.; Academic Press: New York; pp 53–132.

(44) Pabst, G.; Lonez, C.; Vandenbranden, M.; Jestin, J.; Radulescu, A.; Ruysschaert, J. M.; Gutberlet, T. Stalk-free membrane fusion of cationic lipids via an interdigitated phase. *Soft Matter* **2012**, *8*, 7243–7249.

(45) Lewis, R. N.; Winter, I.; Kriechbaum, M.; Lohner, K.; McElhaney, R. N. Studies of the structure and organization of cationic lipid bilayer membranes: calorimetric, spectroscopic, and x-ray diffraction studies of linear saturated P-O-ethyl phosphatidylcholines. *Biophys. J.* **2001**, *80*, 1329–1342.

(46) Pohle, W.; Selle, C.; Gauger, D. R.; Zantl, R.; Artzner, F.; Radler, J. O. FTIR spectroscopic characterization of a cationic lipid-DNA

complex and its components. *Phys. Chem. Chem. Phys.* **2000**, *2*, 4642–4650.

(47) Ryhanen, S. J.; Alakoskela, J. M.; Kinnunen, P. K. Increasing surface charge density induces interdigitation in vesicles of cationic amphiphile and phosphatidylcholine. *Langmuir* **2005**, *21*, 5707–5715.

(48) Pabst, G.; Danner, S.; Karmakar, S.; Deutsch, G.; Raghunathan, V. A. On the propensity of phosphatidylglycerols to form interdigitated phases. *Biophys. J.* **2007**, *93*, 513–525.

(49) Fernandez, R. M.; Lamy-Freund, M. T. Correlation between the effects of a cationic peptide on the hydration and fluidity of anionic lipid bilayers: a comparative study with sodium ions and cholesterol. *Biophys. Chem.* **2000**, *87*, 87–102.

(50) Meidan, V. M.; Glezer, J.; Amariglio, N.; Cohen, J. S.; Barenholz, Y. Oligonucleotide lipoplexes: the influence of oligonucleotide composition on complexation. *Biochim. Biophys. Acta* **2001**, *1568*, 177–182.

(51) Ciani, L.; Ristori, S.; Salvati, A.; Calamai, L.; Martini, G. DOTAP/DOPE and DC-Chol/DOPE lipoplexes for gene delivery: zeta-potential measurements and electron spin resonance spectra. *Biochim. Biophys. Acta* **2004**, *1664*, 70–79.

(52) Ciani, L.; Ristori, S.; Bonechi, C.; Rossi, C.; Martini, G. Effect of the preparation on the structural properties of oligonucleotide/cationic liposome complexes (lipoplexes) studied by electron spin resonance and zeta potential. *Biophys. Chem.* **2007**, *131*, 80–87.

(53) Meidan, V. M.; Cohen, J. S.; Amariglio, N.; Hirsch-Lerner, D.; Barenholz, Y. Interaction of oligonucleotides with cationic lipids: the relationship between electrostatics, hydration and state of aggregation. *Biochim. Biophys. Acta* **2000**, *1464*, 251–261.

(54) Schindler, H.; Seelig, J. EPR spectra of spin labels in lipid bilayers. *J. Chem. Phys.* **1973**, *59*, 1841–1850.

(55) Marsh, D. (1989) in *Spin labeling: Theory and Applications*; Berliner, L. J., Reuben, J., Eds.; Plenum Press: New York; Vol. 8, pp 255–303.

(56) Benatti, C. R.; Barroso, R. P.; Lonez, C.; Ruysschaert, J. M.; Lamy, M. T. DNA alters the bilayer structure of cationic lipid diC14-amidine: a spin label study. *Biochim. Biophys. Acta* **2009**, *1788*, 1304–1309.

(57) Tanaka, T.; Legat, A.; Adam, E.; Steuve, J.; Gatot, J. S.; Vandenbranden, M.; Ulianov, L.; Lonez, C.; Ruysschaert, J. M.; Muraille, E.; Tuynder, M.; Goldman, M.; Jacquet, A. DiC14-amidine cationic liposomes stimulate myeloid dendritic cells through Toll-like receptor 4. *Eur. J. Immunol.* **2008**, *38*, 1351–1357.

(58) Lonez, C.; Vandenbranden, M.; Ouali, M.; Legat, A.; Ruysschaert, J. M.; Elouahabi, A. Free diC14-amidine liposomes inhibit the TNF-alpha secretion induced by CpG sequences and lipopolysaccharides: role of lipoproteins. *Mol. Membr. Biol.* **2006**, *23*, 227–234.

(59) Lonez, C.; Legat, A.; Vandenbranden, M.; Ruysschaert, J. M. DiC14-amidine confers new anti-inflammatory properties to phospholipids. *Cell. Mol. Life Sci.* **2008**, *65*, 620–630.

(60) Wilmar, A.; Lonez, C.; Andrianne, M.; Ruysschaert, J. M.; Vandenbranden, M.; Leo, O.; Temmerman, S. The cationic lipid, diC14-amidine, extends the adjuvant properties of aluminum salts through a TLR-4 and caspase-1 independent mechanism. *Vaccine* **2012**, *30*, 414–424.